HYPERSPECTRAL MIXTURE ANALYSIS USING CONSTRAINED PROJECTIONS ONTO MATERIAL SUBSPACES

John Gruninger , Marsha J. Fox and Robert L. Sundberg
Spectral Sciences, Inc., 99 South Bedford Street, Burlington, MA 01803

ABSTRACT

Hyperspectral imaging sensors provide spectral information related to materials present in each scene pixel. The variability of the natural environment and material conditions makes the extraction of scene material content a difficult problem. We describe a method of mixture analysis that accounts for the variability in material spectra. Each material type identified in the scene is described by a subspace which spans its spectral variability in the scene. An end-member basis is used to define each material subspace. Constrained oblique projections of the pixel spectra onto the material subspaces determines material types and material abundances of the pixels.

1.0 INTRODUCTION

Hyperspectral sensors provide a spectrum for each pixel in a scene that is representative of materials at the surface. Since the number of materials present in the scene is generally small compared to the number of pixels, the spatial resolution of the sensor typically leads to footprints large enough for more than one material to be present in a single pixel. It is desirable to model and interpret the hyperspectral data based on the spectra of the materials and the amounts of the materials present in each pixel. However, the variability of the natural environment and material conditions makes the extraction of scene content a difficult problem. This is often compounded by high correlation among the spectra of the different materials present in a scene. Atmospheric correction can reduce or remove the variability in material spectra due to the water vapor and aerosol contributions but the resultant apparent spectral reflectances still contain variability from other environmental sources. The variability makes it difficult to determine the number of materials present, and adds to the difficulty of determining material abundances, particularly for materials in low abundance in a pixel. The basic tenet of the standard linear mixing model, that one end-member will represent each material, is not typically met in practice and is the primary cause of poor estimates of abundance when variability in the spectra of materials is present.

There have been several efforts to account for the natural variability in material spectra. These include statistical models and modifications to the standard linear mixing model. Statistical approaches treat the scene as a Gaussian mixture model rather than a deterministic mixture of materials. In the Stochastic Expectation Maximization model, a statistical cluster analysis is performed on the scene and the derived clusters are analyzed to obtain estimates of probability distributions. Distributions are defined for constituent and mixed pixel classes.[1,2,3] The approach described in reference 3 has recently been

compared to standard linear mixing model, showing strong correlations between the probabilities of the statistical model and the abundances of the linear mixing model[4]. The Stochastic Mixing Model[5] assumes a linear mix of pixel radiances but defines the composition in a statistical rather than a deterministic formalism. In the Stochastic Mixing Model, mixed pixels are defined by a convex linear combination of pure samples. Hybrid techniques such as AutoSWIR[6,7] perform a statistical clustering on the scene to identify end-member classes and apply a linear mixing model using random sampling to select end-members to generate a distribution of compositions. Bateson *et al.* [8] obtain end-members of a scene by forming a minimum volume simplex. Clusters or bundles of scene pixels are associated with end-members based on their correlation coefficients and a convex hull is formed to represent each bundle. In their approach unmixing is performed using linear programming and minimum and maximum bundle fractions are obtained. In our approach each material type is represented as a convex cone constructed from a basis set of spectra that are representative of the material type. Sets of representative spectra for each material type can be obtained via clustering the pixel spectra or by the generation of end-member spectra. We have taken the latter approach here, using a new hierarchical technique which simultaneously obtains intensity abundance maps for the scene. These abundance maps can be used to determine sets of representative spectra for the material end-members. The sets of representative spectra are processed either by Singular Value Decomposition (SVD), or by convex cone analysis to obtain a basis for each material.[9]

In Section 2, the distinctions between convex hull and convex cone linear mixture modeling are described, and the methodology for performing convex cone mixture modeling for variable material spectra is presented. In Section 3, the approach is applied to data extracted from an AVIRIS scene.

2.0 MIXTURE MODELING

Our notation convention uses bold lower case letters for vectors and bold upper case letters for matrices.

The fundamental convex hull linear mixture model is

$$\mathbf{p} = \mathbf{S}\mathbf{a}$$

where elements of **a** are the fractional contributions of the individual material spectra. The coefficients are required to satisfy the constraints

$$\mathbf{a} \geq \mathbf{0} \text{ and } \sum_A a_A = 1,$$

p is a pixel spectrum from the scene, **S** is a matrix whose columns are end-members, the "pure" material spectra that are present in the scene. The element, a_A, is the fractional contribution of the spectrum of material A to the pixel spectrum. In addition to the direct interpretation, the coefficients, a_A , are often attributed to geometric fill factors and material abundance in the pixel. The basic underlying assumptions of the convex-hull linear mixing model include:

(1) A single spectrum, or end-member is adequate to represent a material,

(2) Linear mixtures of the material spectra model the spectrum of a mixture of the materials.

In most natural scenes, assumption (1) is not met. Radiant energy at the sensor is a non-linear mixture of atmospheric and material radiance contributions. Even if the data has been atmospherically corrected, there are still variations in the apparent reflectance of a material surface due to effects of varying environment, illumination and natural variations and conditions of materials. When these variations are not taken into account, the coefficients , a_A , no longer reflect the true fill factors. Forcing the coefficient to sum to one does not rectify the situation and provides a poorer fit to the pixel reflectance or radiance. The reduced degree of freedom introduced by the constraint can be made up by adding an additional pseudo-material to the basis. Strategies center around the addition of a dark or zero reflectance end-

member as an extreme vector in defining the simplex.[10] These dark end-members let the coefficients satisfy the constraints, with the abundance of shade filling the gap when material end-members would freely sum to less than one. However this does not solve the problem of a pixel for which the material end-members would freely sum to greater than one, nor do the resulting fractional contributions necessarily represent the actual fill factors or abundances.

The convex cone linear mixture model is given by

$$\mathbf{p} = \mathbf{Sf}$$

$$\mathbf{f} \geq \mathbf{0}$$

where the elements of **f** are the actual contributions of the material end-member spectra to the pixel spectrum, not fractional contributions as before. The coefficients satisfy the positivity constraint but their sum in not restricted. The inequality constraint, ensures that the end-member spectra are added positively. With the sum to one constraint no longer applied, the additional degree of freedom leads to a better fit to pixel radiance. In the convex cone approximation, the interpretation of the coefficients can be made in terms of fractional contributions to the total radiance or reflectance. Summing the channel radiances in the mixed pixel and end-member spectra leads to

$\sum_A I_A f_A = I_{Pixel}$, where I_{Pixel} is the sum of the channel radiances in the pixel and I_A is the sum of the channel radiances in the A^{th} end-member spectrum. The equality is in the least squares sense assuming that the channel residuals sum to zero. The fractional contribution of radiance from end-member *A* to the pixel radiance is, the quantity $I_A f_A / I_{Pixel}$. Note that this relation holds regardless of whether the sum to one constraint is applied and active.

Formation of the Material End-member Basis

To obtain an estimate of the pixel fill or material abundance in the pixel, it is necessary to address the variability in material spectra that exists in the scene. We include the variability in the material spectra by the inclusion of an end-member basis for each material. A necessary condition for the coefficients in a linear model to correspond to pixel fills is for all pure material spectra to be modeled by a mix of the end-member spectra with coefficients summing to one. If this is met, the sum of pure material contributions to a mixed pixel can match its actual abundance in the pixel and the total sum of material abundances can freely approach one. The underlying assumption here is that the subtle spectral variations of the various manifestations of the "material" in the scene correlate with its intensity variations. Then a careful estimate of the spectral shape of the material contributions will map with both the fractional intensity and the abundance or fill factor.

First, sets of pixel spectra which can be identified as belonging to the same material and which span the variability need to be found. These can be obtained by performing a standard clustering of the pixel spectra, or alternatively a clustering of the fractional abundance data provided by a preliminary convex cone analysis. Either results in the selection of sets of highly correlated spectra which are representative of single materials or material types. The set of spectra for material *A* form a matrix, $\mathbf{P}_A$, whose columns are the individual pixel spectra.

Next, a basis for each pure material, is determined from the clustered pixels. Two approaches to finding a basis for each pure material have been undertaken. One based on singular value decomposition and one based on output of a convex cone analysis.

A singular value decomposition can be performed on the set of clustered pixels to obtain a basis from the left singular vectors.

$$\mathbf{P}_A = \mathbf{U}_A \boldsymbol{\eta}_A \mathbf{V}_A^T$$

where $\mathbf{P}_A$ is the matrix of representative pixel spectra of material A, $\mathbf{U}_A$ is the matrix of left singular vectors, ς_A is a diagonal matrix of singular values and $\mathbf{V}_A$ is the matrix of right singular vectors. Since the pixel spectra of the material are highly correlated , only a few of the singular values will be significant and the expansion can be truncated to only a few basis functions. The matrix of coefficients, $\mathbf{Q}_A$, for the singular vector expansion of $\mathbf{P}_A$ is given by

$$\mathbf{Q}_A = \boldsymbol{\varsigma}_A \mathbf{V}_A^T$$

Since the singular vectors form orthogonal matrices, the decomposition can be easily inverted to express the left singular vectors as an expansion in the original set of pixel spectra,

$$\mathbf{U}_A = \mathbf{P}_A \mathbf{V}_A \boldsymbol{\varsigma}_A^{-1}$$

For a single pixel spectrum of material A , the expansion coefficients are given by

$$\mathbf{p}_A = \mathbf{U}_A \mathbf{q}_A = \mathbf{P}_A (\mathbf{V}_A \boldsymbol{\varsigma}_A^{-1} \mathbf{q}_A)$$

If the pixel spectrum, $\mathbf{p}_A$, is one of the columns of $\mathbf{P}_A$, and the SVD has not been truncated too severely, the transformed coefficients of the vector, $\mathrm{V}_A \boldsymbol{\varsigma}_A^{-1} \mathrm{q}_A$, sum to one (one of the coefficients is one and the others are zero). Provided that the basis spans all scene pixels of material A, the expansion coefficients of material A pixels will sum closely to one. The individual coefficients for the contributions of the columns of $\mathbf{P}_A$ are not well estimable due to the high correlation among columns, however, the linear combinations of the columns that lie in the subspace of the dominant singular vectors, are estimable[11]. The sums which are the desired quantities are estimable.

The alternative approach to determining a basis, is to use an end-member procedure to find the extreme vectors of each set of representative spectra. The Sequential Maximum Angle Convex Cone (SMACC) program[9], uses a convex cone matrix factorization algorithm to find a hierarchy of end-members and simultaneously finds the fractional contribution to intensity maps of each material represented in the basis and a set of residuals for all pixels. It can be used to find sets of representative spectra for each end-member material, and for each of these sets be reapplied to find a convex cone basis. The basis will be the set of extreme vectors of the set $\mathbf{P}_A$. For all pixel spectra of material A which lie within the cone, the expansion coefficients will sum to closely to one.

Once a basis for each material has been determined, the convex cone mixing model can be applied to mixed pixels do determine abundances or fill factors. For a mixed pixel spectrum, $\mathbf{p}$,

$$\mathbf{p} = \mathbf{B}\mathbf{q}$$

where $\mathbf{B}$ is partitioned into sub-matrices of columns for each material

$$\mathbf{B} = \{\mathbf{B}_A, \mathbf{B}_B, \ldots\}.$$

The column vector $\mathbf{q}$ of expansion coefficients is partitioned into sub-vectors of $\{\mathbf{q}_A, \mathbf{q}_B, \ldots\}^T$. In general, each material can have its own subspace. We restrict the subspaces to convex cones by requiring positive contributions of the material spectra to the mixed pixel. For all materials $\{A\}$ with a convex cone basis, the constraints is that all components of the expansion vectors for each material be positive, $\mathrm{q}_A \geq 0$. For all materials $\{B\}$ with a singular vector basis, the necessary constraint is that all components of the vectors transformed expansion vectors for each material be positive, $\mathrm{V}_B \boldsymbol{\varsigma}_B^{-1} \mathrm{q}_B \geq 0$. These constraints confine the bases to the cones which span the variability of the material spectra as represented in the clusters of materials ,$\mathbf{P}_A$, $\mathbf{P}_B$, etc.

Estimates of the abundance of fill factor for a material is obtained by accumulating the contributions from each basis representing the material. If the basis is a convex cone, the abundances are obtained from the sum of the expansion coefficients for the basis representing that material,

$$a_A = \sum_k^{n_A} q_A(k)$$

where n_A is the number of basis vectors for the cone. For materials whose bases are orthogonal singular vectors, the abundance of that material in the mixed pixel is given by the sum of the transformed expansion coefficients,

$$a_B = \sum_k^{n_B} \mathrm{V}_B \boldsymbol{h}_B^{-1} q_B(k)$$

where n_B is the number of singular vectors chosen to represent material *B*.

The coefficients in the linear model are constrained to so that the mixed pixel abundances are determined by the constrained oblique projections of the mixed pixel spectrum onto the convex cones of the basis representations for each material. The sum of the abundances can be constrained to sum to one. However a measure of the quality of the model is how close the free summation is to one. Causes for failure include: a material in the pixel that is missing from the model, a definition of "material" that is too broad so that correlations between spectral shape variations and intensity are weak, and an inadequate basis representation that fail to span some of the pure material spectra that exist in the data. Inspection of the values of the free summations help determine the adequacy of the model.

3.0 APPLICATION

Portions of an AVIRIS hyperspectral datacube taken at Stennis AFB, shown in Figure 1, were analyzed using SMACC. First, 100 end-members in a hierarchy were determined. The first few are shown in Figure 2. In Figure 3, fractional contributions to intensity of the first few end-members for the sub-cube shown in Figure 1. are shown, in which the vegetation, road, building are clearly separated. We used these fractional intensity maps to select representative sets of spectra for the road and vegetation. Although there are no obvious deep shadows in the scene, there is partial shadowing and variability in both the vegetation and road material. The variations in the spectra are shown in Figures 4a and 4b. The spectra in the figures represent the extremes of the variations found in the first 100 "end-members" of the hierarchy. The first end-member selected for vegetation and road bracket the spectra from above and below respectively in Figures 4a and 4b. Singular value decomposition basis sets were derived for the materials and end-member basis sets were determined. In calculations of abundance, these were constrained to span a convex cone. Not having ground truth, we synthesized mixtures of road and vegetation from pixel spectra selected from the extreme groups shown above. We used the spectra within the variation bounds of Figures 4a and 4b to form mixtures ranging from 100% road to 100% vegetation These spectra were excluded from the representative sets used to form the SVD bases and the end-member bases. In order to obtain a basis which will predict abundances accurately, an initial test is that they predict pure material with coefficients freely summing to close to one. For the road material this required two basis functions. For the vegetation, a larger basis, of 6 singular vectors or was required to accommodate all the spectra shown in Figure 4a. These are the most varied of the vegetation spectra present in the scene. It required the use of four of them as end-members to achieve the desired result. However for the large majority of vegetation spectra in the scene, two basis functions were adequate. We used a quadratic programming algorithm[12] to perform the constrained least squares calculations on the synthetic mixtures. Calculations were performed for each mixture. These included one end-member per material calculations using both the standard convex hull and convex cone mixing models. Also convex cone mixing model with singular vector and convex cone basis sets for vegetation and road was applied to each mixture. In all cases the

contributions of all spectra were required to be positive. Results of these calculations are illustrated in Figure 5. The "unknown" vegetation spectra has a mean reflectance of approximately 80% of the 1st end-member, while the mean reflectance of the "unknown" road spectrum is approximately 108% of the 1st road end-member. In addition to the subtle spectral shape changes, the overall brightness of the spectrum plays a large role in the behavior of the one end-member per material models. In the one end-member per material convex cone model the abundance coefficients are required to be positive but have no constraint on their sum. The abundances predicted by the model roughly track the true values but reflect the differences in mean radiance. True 100% vegetation is predicted at with an abundance coefficient of .8 with the road contribution at 0., while true 100% road is predicted with coefficient of approximately 1.10 with vegetation abundance coefficient of .03. These predictions are not good for abundance. Requiring the additional constraint on these coefficients of summing to one does little to improve the results. Both of the single end-member per material methods do poorly at detecting vegetation in the mixtures until it is present at the 20% level. The sum to one constraint causes the standard linear mixing model to not detect road until it is present at about 10%. The convex cone mixing model with a basis set for each material is much more responsive to small amount of material and performs well over the entire concentration range.

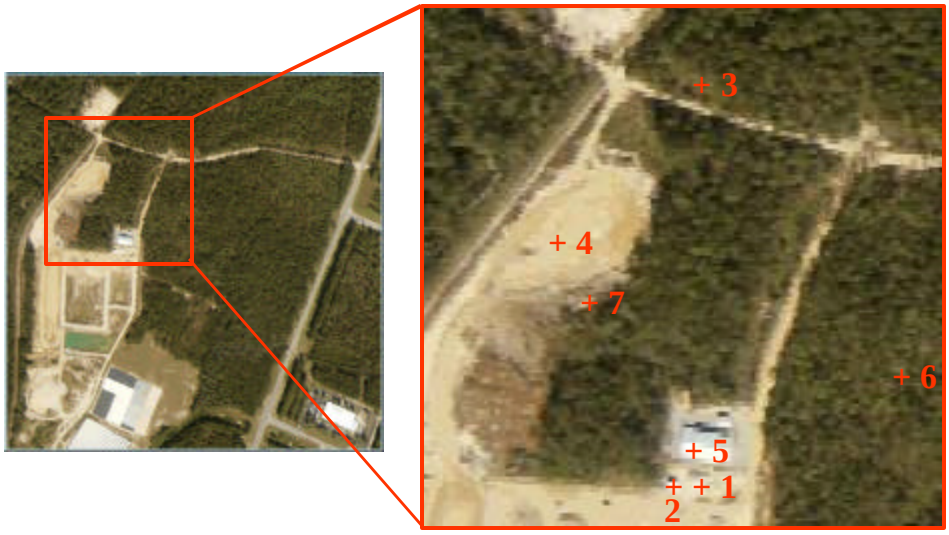

Figure 1. AVIRIS Stennis scene used for the application with sub-window selected for analysis. The pixel locations of the first seven end-members selected by SMACC.

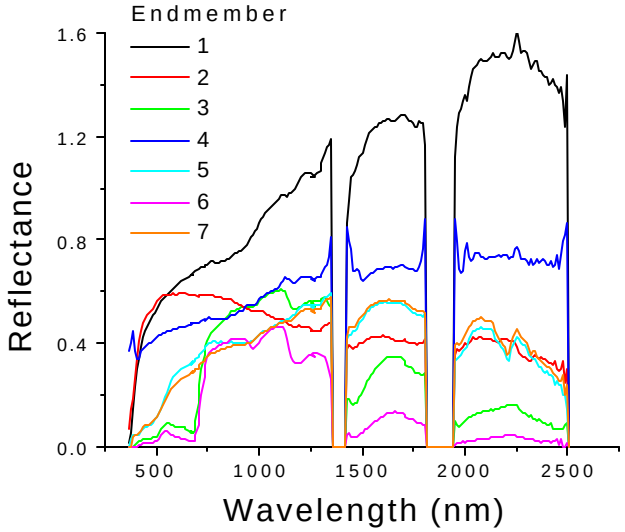

Figure 2. The first seven end-member spectra of the sub window as selected by SMACC.

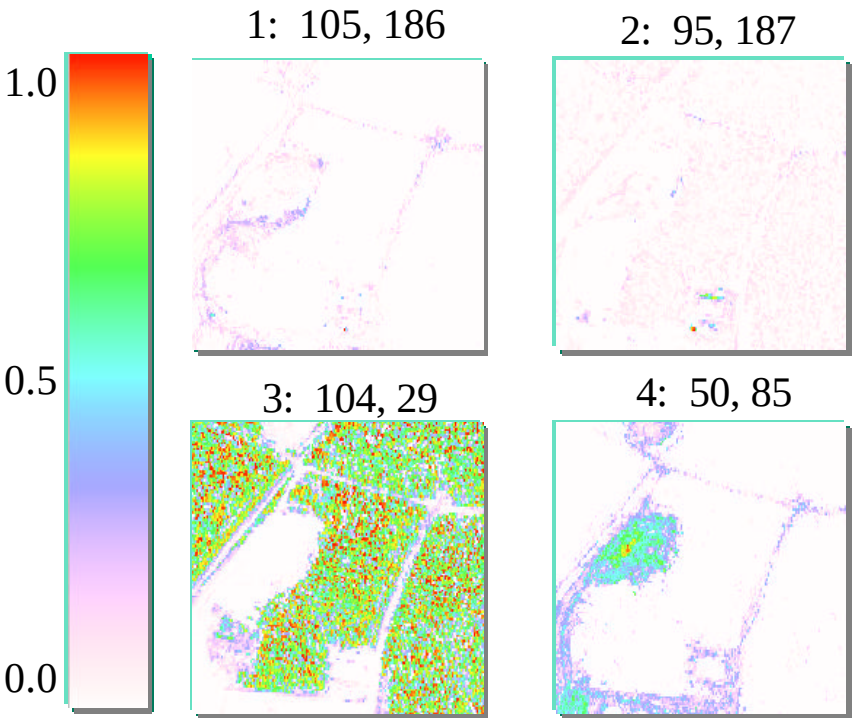

Figure 3. Fractional intensity maps for the first four end-members. End members three and for are the first endmembers selected for vegetation and road respectively.

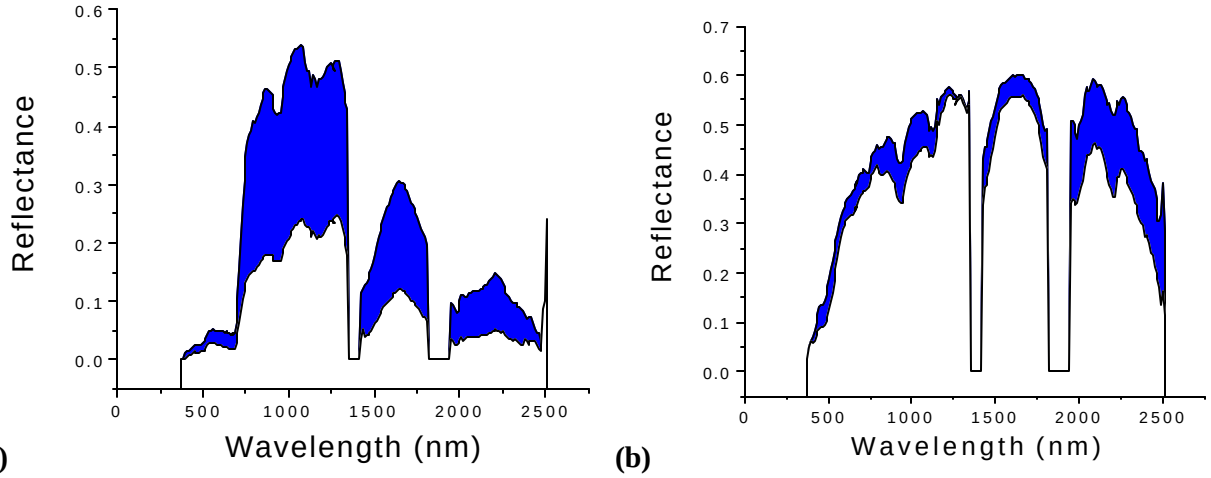

(a) **(b)**

Figure 4. Figure 4a shows the variability of vegetation spectra in the scene. Figure 4b shows the variability of the road spectra in the scene. The spectra chosen were selected from the first 100 "end-members" as selected by SMACC.

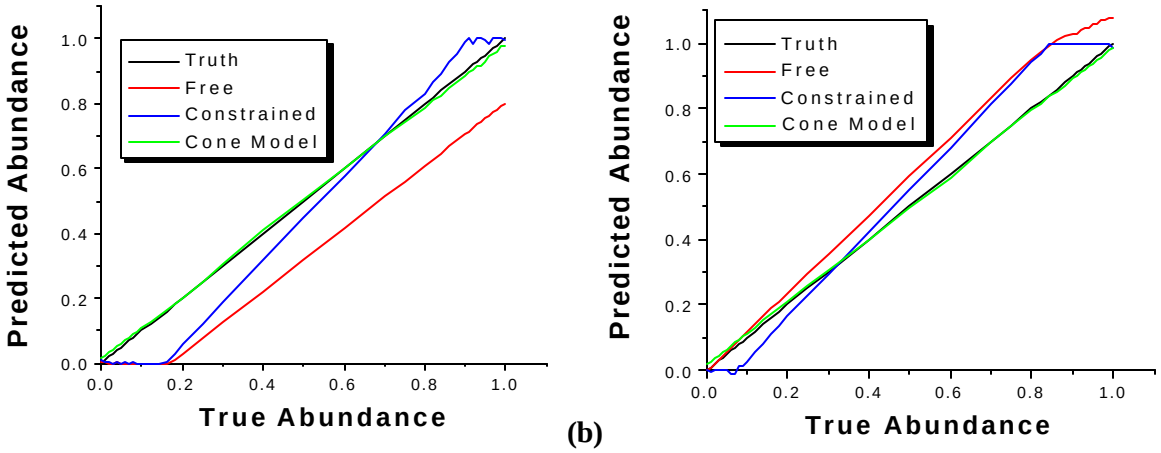

Figure 5. Plots of truth versus model calculations of pixel abundance. Calculations labeled constrained are for the standard linear mixing model using one end member per material. Calculations labeled free are single end-member calculations without the sum to one constraint. Calculations labeled cone are for the results using convex cones to represent both materials. Figure 5a contains the calculated abundances for the vegetation. Figure 5b contains calculated abundances for the road.

4.0 CONCLUSIONS

The method presented appears to be a viable approach to determining material abundance in mixed pixels when there is variability in individual material spectra. Representation of a material by a basis which spans its variability leads to an accurate description of mixed pixels with estimates of abundance, and spectral shape of the individual material contributions. The constrained projections which restrict the bases to span convex cones rather than the entire subspace reduces overlap among the different materials. The increase in size of the overall basis for the modeling of the scene requires care to avoid over-fitting which will result from the model matrix, **S**, becoming ill-conditioned.

Using singular vectors to represent the variations of a material results in each material being represented by an orthogonal basis, however the overlap among materials increases as the convex cones broaden to span the individual material variations. It will be possible to utilize regularization techniques, and the constraints help to reduce the tendency of all small coefficients increasing with regularization. However the simpler approach may be to first perform a preliminary analysis using single end-members and to use the resulting fractional contribution intensity maps, and the materials found present in the mixed pixels, to define the appropriate subset of materials for modeling the mixed pixels in boundary regions.

The convex cone mixture modeling technique can be exercised whenever it is important to know abundances, particularly when it is important to know small abundances where the simpler one end-member per material estimates are the most sensitive to error.

ACKNOWLEDGMENTS

This work was supported support by Spectral Sciences, Inc. AFRL/SN under Contracts F33615-00-C-1600 and F33615-99-C-1469. We also acknowledge AFRL/VS for support for preliminary development of SMACC.

REFERENCES

1. T. K. Moon, "Expectation-Maximization Algorithm", IEEE Signal processing Magazine, Vol 13, No.6 (November 1996).
2. R. A. Redner and H. F. Walker, "Mixture Densities, Maximum Likelihood, and EM Algorithm", SIAM Review, Vol. 26 No. 2 (April 1984).
3. P. Masson and W. Pieczynski, "SEM Algorithm and Unsupervised Statistical Segmentation of Satellite Images", *IEEE Transactions on Geosci. And remote Sensing,* **31**,No. 3 (May 1993).
4. S. Beaven, L. E. Hoff and E. M. Winter, "Comparison of SEM and linear Unmixing Approached for Classification of Spectral Data", *Proceedings SPIE* **3753**, Imaging Spectrometry V,300-307,(1999)
5. Alan D. Stocker and Alan P.Shaum, "Application of Stochastic Mixing Models to Hyperspectral Detection Problems", *Proceedings SPIE* **3071**, Algorithms for Multispectral and Hyperspectral Imagery III,47-60, (1997).
6. G. P. Asner and D. B. Lobell, "A Biogeophysical Approach to Automated SWIR Unmixing of Soils and Vegetation", *Remote Sens. Environ*., **74**, 99-112,(2000).
7. David B. Lobell, Gregory P. Asner, Beverly E. Law and Robert N. Treuhaft, "Subpixel Canopy Cover Estimation of Coniferous Forests in Oregon using SWIR Imaging Spectrometry", *JGR* **106** D6, 5151-5160 (2001).
8. C. Ann Bateson, Gregory P. Asner, and Carol A. Wessman, "End-member Bundles: A New Approach to Incorporating End-member Variability into Spectral Mixture Analysis", *IEEE Transactions on Geosci. and Remote Sensing,* **38**, 1083-1094, (2000).
9. J. Gruninger, R. L. Sundberg, M. J. Fox, R. Levine, W. F. Mundkowsky, M. S. Salisbury and A. H. Ratcliff, "Automated Optimal Channel Selection for Spectral Imaging Sensors", *Proceedings SPIE* **4381**, Algorithms for Multispectral and Hyperspectral Imagery VII,[4381-07], (2001).
10. M. D. Craig, "Minimum-Volume Transformations for Remotely Sensed Data", *IEEE Trans. Geoscience and Remote Sensing*, **32**, 99-109, (1994).
11. S. D. Silvey "Multicollinearity and Imprecise Estimation", Royal Statistical Soc., Series B, **31**, 539-552, (1969)
12. Lawson, Charles. L, and Hanson, Richard J., "Solving Least Squares Problems", Prentice Hall Englewood Cliffs New Jersey, (1974).